

# Efficient generation of periodic and quasi-periodic non-diffractive optical fields with phase holograms

Victor Arrizón,\* David Sánchez-de-la-Llave, Guadalupe Méndez, and Ulises Ruiz  
*Instituto Nacional de Astrofísica, Óptica y Electrónica, Apartado Postal 51 y 216, Puebla PUE 72000, México*  
*\*arrizon@inaoep.mx*

**Abstract:** The superposition of multiple plane waves with appropriate propagation vectors generates a periodic or quasi-periodic non-diffractive optical field. We show that the Fourier spectrum of the phase modulation of this field is formed by two disjoint parts, one of which is proportional to the Fourier spectrum of the field itself. Based on this result we prove that the non-diffractive field can be generated, with remarkable high accuracy and efficiency, in a Fourier domain spatial filtering setup, using a synthetic phase hologram whose transmittance is the phase modulation of the field. In a couple of cases this result is presented analytically, and in other cases the proof is computational and experimental.

©2011 Optical Society of America

**OCIS codes:** (090.1760) Computer holography; (070.3185) Invariant optical fields; (050.5298) Photonic crystals; (230.6120) Spatial light modulators.

---

## References and links

1. J. P. Kirk and A. L. Jones, "Phase-only complex-valued spatial filter," *J. Opt. Soc. Am.* **61**(8), 1023–1028 (1971).
2. R. W. Cohn and M. Liang, "Approximating fully complex spatial modulation with pseudorandom phase-only modulation," *Appl. Opt.* **33**(20), 4406–4415 (1994).
3. J. A. Davis, D. M. Cottrell, J. Campos, M. J. Yzuel, and I. Moreno, "Encoding amplitude information onto phase-only filters," *Appl. Opt.* **38**(23), 5004–5013 (1999).
4. M. A. A. Neil, T. Wilson, and R. Juskaitis, "A wavefront generator for complex pupil function synthesis and point spread function engineering," *J. Microsc.* **197**(3), 219–223 (2000).
5. V. Arrizón, G. Méndez, and D. Sánchez-de-La-Llave, "Accurate encoding of arbitrary complex fields with amplitude-only liquid crystal spatial light modulators," *Opt. Express* **13**(20), 7913–7927 (2005), <http://www.opticsinfobase.org/oe/abstract.cfm?URI=oe-13-20-7913>.
6. V. Arrizón, U. Ruiz, R. Carrada, and L. A. González, "Pixelated phase computer holograms for the accurate encoding of scalar complex fields," *J. Opt. Soc. Am. A* **24**(11), 3500–3507 (2007).
7. V. Arrizón, D. Sánchez-de-la-Llave, U. Ruiz, and G. Méndez, "Efficient generation of an arbitrary nondiffracting Bessel beam employing its phase modulation," *Opt. Lett.* **34**(9), 1456–1458 (2009).
8. J. Durmin, "Exact solutions for nondiffracting beams. I. The scalar theory," *J. Opt. Soc. Am. A* **4**(4), 651–654 (1987).
9. G. Indebetouw, "Nondiffracting optical fields: some remarks on their analysis and synthesis," *J. Opt. Soc. Am. A* **6**(1), 150–152 (1989).
10. S. Chávez-Cerda, M. A. Meneses-Nava, and J. M. Hickmann, "Interference of traveling nondiffracting beams," *Opt. Lett.* **23**(24), 1871–1873 (1998).
11. J. Molloy and M. Padgett, "Lights, action: optical tweezers," *Contemp. Phys.* **43**(4), 241–258 (2002).
12. K. Dholakia, P. Reece, and M. Gu, "Optical micromanipulation," *Chem. Soc. Rev.* **37**(1), 42–55 (2007).
13. M. Dienerowitz, M. Mazilu, and K. Dholakia, "Optical manipulation of nanoparticles: a review," *J. Nanophotonics* **2**(1), 021875 (2008).
14. K. Volke-Sepúlveda and R. Jáuregui, "All-optical 3D atomic loops generated with Bessel light fields," *J. Phys. At. Mol. Opt. Phys.* **42**(8), 085303 (2009).
15. P. Xie and Z. Q. Zhang, "Multifrequency gap solitons in nonlinear photonic crystals," *Phys. Rev. Lett.* **91**(21), 213904 (2003).
16. D. Neshev, E. Ostrovskaya, Y. Kivshar, and W. Krolikowski, "Spatial solitons in optically induced gratings," *Opt. Lett.* **28**(9), 710–712 (2003).
17. J. Xavier, P. Rose, B. Terhalle, J. Joseph, and C. Denz, "Three-dimensional optically induced reconfigurable photorefractive nonlinear photonic lattices," *Opt. Lett.* **34**(17), 2625–2627 (2009).

18. J. Xavier, M. Boguslawski, P. Rose, J. Joseph, and C. Denz, "Reconfigurable optically induced quasicrystallographic three-dimensional complex nonlinear photonic lattice structures," *Adv. Mater. (Deerfield Beach Fla.)* **22**(3), 356–360 (2010).
19. W. D. Mao, J. W. Dong, Y. C. Zhong, G. Q. Liang, and H. Z. Wang, "Formation principles of two-dimensional compound photonic lattices by one-step holographic lithography," *Opt. Express* **13**(8), 2994–2999 (2005), <http://www.opticsinfobase.org/oe/abstract.cfm?URI=oe-13-8-2994>.
20. V. Arrizón, S. Chavez-Cerda, U. Ruiz, and R. Carrada, "Periodic and quasi-periodic non-diffracting wave fields generated by superposition of multiple Bessel beams," *Opt. Express* **15**(25), 16748–16753 (2007), <http://www.opticsinfobase.org/oe/abstract.cfm?URI=oe-15-25-16748>.
21. SLM HEO 1080 P, HOLOEYE Photonics AG.

## 1. Introduction

Generation of an arbitrary optical field is a significant and useful task in physical optics. It requires spatially variable independent modulation of both the amplitude and the phase of the field. Although a general solution to this problem is provided by synthetic holography, both the efficiency and the accuracy of the method are highly dependent on the hologram type and the field to be generated [1–7].

Non-diffractive optical fields (NDOFs) have drawn the attention of researchers over the last two decades. Besides the attractiveness of these fields from a theoretical point of view [8–10], they have been investigated in applications such as atom and particle trapping [11–14] and generation of nonlinear wave guides [15,16]. A great variety of NDOFs can be obtained by superposing multiple plane waves whose propagation vectors have a common component respect to the propagation axis. In particular, if the transverse projections of the waves' propagation vectors have uniformly distributed azimuth angles we obtain a periodic or quasi-periodic NDOF. Fields of this type are useful to generate photonic crystals and quasi-crystals in different optical media [17,18]. In the following sections we use the acronym NDOF to refer only to periodic or quasi-periodic fields.

The multiple waves required to generate a NDOF can be obtained using beam splitters and mirrors. However, the implementation of this method is quite difficult, mainly if specific phase shifts need to be applied to the interfering waves [19]. Here we discuss a simple and robust technique to generate these fields, based on synthetic holography. We show that the Fourier spectrum of the phase modulation of a NDOF is formed by two disjoint parts, one of which is proportional to the Fourier spectrum of that field. This property is of the utmost importance in synthetic holography. Based on it we prove that a synthetic phase hologram (SPH) whose transmittance is the phase modulation of a NDOF can be employed to accurately generate this field with remarkable high efficiency, in a Fourier domain spatial filtering setup. For further reference this SPH is referred to as kinoform of the NDOF. The above mentioned result is proved analytically when the number of interfering waves is 2 and 4. In other cases, the result is proved numerically and experimentally. In addition, it is noted that the NDOF becomes a non-diffracting Bessel beam when the number of interfering waves tends to infinity. In this case, the result has been proved in Ref [7].

## 2. Theory

A NDOF can be expressed by the superposition of  $Q$  plane waves of equal amplitude, whose propagation vectors have a common projection  $k_z$  respect to the  $z$ -axis. The transverse component modulus of the propagation vectors,  $k_t$ , is also a constant, given by the identity  $k_t^2 = k^2 - k_z^2$ , where  $k = 2\pi/\lambda$  is the wave number. As a particular interesting case, we assume that the projection of the propagation vectors of interfering waves to the  $x$ - $y$  plane form angles, respect to the  $x$ -axis, which are multiple of  $2\pi/Q$ . These interfering plane waves can be modulated by different constant phase shifts. Thus, the NDOF formed by the superposition of the  $Q$  plane waves can be expressed as

$$f(r, \theta) = C \sum_{n=0}^{Q-1} \exp(i\theta_n) \exp[i2\pi\rho_0 r \cos(\theta - n\Delta\theta)], \quad (1)$$

where  $r$  and  $\theta$  are the radius and angle of the cylindrical coordinates system, respectively, and  $\rho_0$  is a spatial frequency, given by  $k_r/2\pi$ . Equation (1) represents the NDOF at the plane  $z = 0$  since we have omitted the propagation factor  $\exp(ikz)$ . Although the phase shift for the  $n$ -th plane wave can be arbitrary, we will consider only the linear phase shift  $\theta_n = p(n\Delta\theta)$ , where  $\Delta\theta = 2\pi/Q$ , and  $p$  is an integer number that represents topological charge. The normalization constant  $C$  makes the maximum of  $|f(r,\theta)|$  equal to 1. In particular, it is found that  $C = 1/Q$  if the topological charge is  $p = 0$ . As illustration, amplitudes and phases of NDOFs with parameters ( $Q = 5, p = 0$ ) and ( $Q = 6, p = 1$ ) are displayed in Fig. 1. Every non diffracting field can be expressed in a base of non diffracting Bessel beams  $BB_q(r,\theta) = J_q(2\pi\rho_0r)\exp(iq\theta)$  [9]. In connection with this result, Arrizón et al pointed out that the NDOF in Eq. (1) is equivalent to the sum of all the Bessel beams  $BB_q(r,\theta)$  of orders  $q = NQ + p$ , where  $N$  is an arbitrary integer number [20].

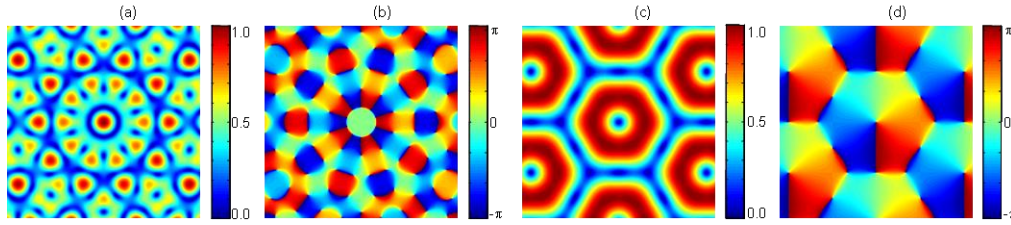


Fig. 1. Partial view of (a) the modulus and (b) the phase of the NDOF with parameters ( $Q = 5, p = 0$ ). The modulus and the phase of the NDOF with parameters ( $Q = 6, p = 1$ ) are respectively shown at parts (c) and (d) of the figure.

For convenience, in the following analysis we will express the NDOF in rectangular coordinates by the function  $h(x,y)$ . If we were able to implement a transmission function with the mathematical form of the complex amplitude of the NDOF, it would generate this field with efficiency

$$\eta_f = \frac{\int_{\Omega} |h(x,y)|^2 dx dy}{\int_{\Omega} dx dy}, \quad (2)$$

where the integration domain  $\Omega$  is the support (or pupil) that physically limits the field. Expressing the NDOF in the polar form  $h(x,y) = |h(x,y)|\exp[i\phi(x,y)]$ , its kinoform is given by

$$h_k(x,y) = \exp[i\phi(x,y)]. \quad (3)$$

It is possible to relate  $h(x,y)$  and  $h_k(x,y)$  by the expression

$$h_k(x,y) = \beta h(x,y) + e(x,y), \quad (4)$$

where  $\beta$  is a positive constant, referred to as amplitude gain, and  $e(x,y)$  is the hologram modulation error. Denoting the Fourier transforms of  $h(x,y)$  and  $e(x,y)$  by  $H(u,v)$  and  $E(u,v)$ , respectively, the Fourier transform of the kinoform is given by  $H_k(u,v) = \beta H(u,v) + E(u,v)$ . The condition required to obtain the complex function  $h(x,y)$  from its kinoform  $h_k(x,y)$  is to have a null overlapping of functions  $H(u,v)$  and  $E(u,v)$ . For further reference, this requirement is referred to as kinoform spectrum condition. If this condition is fulfilled, the complex field  $h(x,y)$  is obtained by conventional spatial filtering, applied to the Fourier spectrum  $H_k(u,v)$ , and an additional Fourier transform operation. In this case the field  $h(x,y)$  is generated from its kinoform with efficiency  $\eta_k = \beta^2 \eta_f$ . The efficiency gain of the kinoform, respect to the efficiency of the complex transmittance [Eq. (2)] is given by

$$G_k = \eta_k / \eta_f = \beta^2. \quad (5)$$

In conventional SPHs designed to generate arbitrary optical fields the best efficiency gain is equal to 1 [1–3,6]. However, SPHs designed for generation of special complex fields can

provide an efficiency gain larger than 1. An example is a SPH applied to the specific task of generating arbitrary high order Bessel beams [7]. An important result, that we will prove next, is that the efficiency gain  $G_K$  is also larger than 1 when the NDOF defined in Eq. (1) is implemented using its kinoform. Moreover, we will prove that it is possible to obtain a perfect spatial isolation of the terms  $H(u,v)$  and  $E(u,v)$  in the kinoform Fourier spectrum, allowing an accurate generation of the field  $h(x,y)$ , by spatial filtering. Although the NDOF is generated displaying only its phase modulation in a SLM, it must be recognized that the amplitude information of the NDOF is in some way provided by the structure of the binary spatial filter, which is designed to transmit only the information of the NDOF at the Fourier domain of the kinoform.

### 2.1. Generation of NDOFs using their kinoforms

A first illustrative case that we consider is the periodic NDOF with parameters ( $Q = 2, p = 0$ ), whose modulation is  $h(x,y) = \cos(2\pi\rho_0x)$ . The kinoform of this real valued function is given by its sign, which is depicted in Fig. 2. It is straightforward to express the transmittance of this kinoform by the Fourier series

$$h_K(x, y) = \sum_{m=1}^{\infty} c_m \cos[2\pi(m\rho_0)x] \quad (6)$$

with coefficients  $c_m = 4/(m\pi)$  for odd  $m$  and  $c_m = 0$  otherwise. The series in Eq. (6) is transformed into the expression in Eq. (4), with an amplitude gain  $\beta = c_1 = 4/\pi$ , and an error  $e(x,y)$  formed by multiple harmonics of the NDOF  $\cos(2\pi\rho_0x)$ . This composition of the error allows the isolation of  $H(u,v)$  and  $E(u,v)$  in the Fourier domain of  $h_K(x,y)$ . The efficiency gain of this kinoform is  $G_K = \beta^2 = (4/\pi)^2$ , which is clearly larger than 1. Although the efficiency gain, can be larger than 1 (as is the case in the above example) the efficiency of the hologram itself, given by  $\eta_K = \beta^2\eta_f$ , is always smaller or equal than 1. The efficiency of the complex transmittance that generates the field  $h(x,y) = \cos(2\pi\rho_0x)$  is [according to Eq. (2)]  $\eta_f = 1/2$ , and the efficiency of the kinoform is  $\eta_K = 8/\pi^2 \approx 0.81$ .

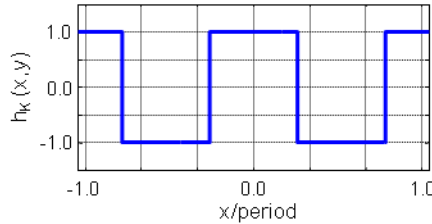


Fig. 2. Modulation of the kinoform for the one dimensional NDOF  $\cos(2\pi\rho_0x)$ .

The second example is the NDOF with parameters ( $Q = 4, p = 0$ ). In this particular case, to simplify the analysis, we add a phase shift  $\pi/4$  to the coordinate  $\theta$ , and the NDOF can be expressed as

$$h(x, y) = \frac{1}{2} \cos[\sqrt{2}\pi\rho_0(x + y)] + \frac{1}{2} \cos[\sqrt{2}\pi\rho_0(x - y)]. \quad (7)$$

The modulus and phase in the basic cell of this NDOF are displayed in Figs. 3(a) and 3(b). The normalized modulus of the Fourier spectrum  $H(u,v)$ , displayed in Fig. 3(c), shows 4 spots, which correspond to the 4 interfering plane waves. The size and form of these spots is determined by the finite pupil that limits the field  $h(x,y)$ . In this and other numerical simulations we employ a circular pupil of radius  $R = 7.5\rho_0^{-1}$ . Applying simple trigonometric relations, the NDOF can be expressed in separable form

$$h(x, y) = \cos[\sqrt{2}\pi\rho_0x] \cos[\sqrt{2}\pi\rho_0y]. \quad (8)$$

Employing this expression it is possible to represent the kinoform  $h_K(x,y)$  by the product of two one-dimensional kinoforms of cosine functions. Thus, considering the analytical Fourier series in Eq. (6), the kinoform of the field in Eq. (8) is given by the 2D Fourier series

$$h_K(x,y) = \sum_{m=1}^{\infty} \sum_{q=1}^{\infty} c_{mq} h(mx, qy) \quad (9)$$

with coefficients  $c_{mq} = 16/(mq\pi^2)$ , for odd  $m \times q$ , and  $c_{mq} = 0$ , otherwise. The series in Eq. (9) can be reduced to the relation in Eq. (4), with amplitude gain  $\beta = c_{11} = 16/\pi^2$ , and error  $e(x,y)$  formed by harmonics of the NDOF  $h(x,y)$ . Again, this composition of  $e(x,y)$  allows the perfect separation of the terms  $H(u,v)$  and  $E(u,v)$  in the Fourier domain of  $h_K(x,y)$ . The efficiency gain of this kinoform is  $G_K = \beta^2 = 256/\pi^4$ , which is even larger than the gain obtained in the previous one-dimensional case. With this value of  $\beta$  we obtain the error function  $e(x,y) = h_K(x,y) - \beta h(x,y)$  and its Fourier spectrum  $E(u,v)$ . The modules of the Fourier spectra  $H_K(u,v)$  and  $E(u,v)$  are displayed in Figs. 3(d) and 3(e). The values in the color-bars of these Fourier spectra images are normalized respect to the peak value in  $|H(u,v)|$  [Fig. 3(c)]. Similar normalization is applied to the Fourier spectra of functions in further examples. It is clearly noted in parts (c) and (e) of Fig. 3 that  $E(u,v)$  presents null overlapping with  $H(u,v)$ .

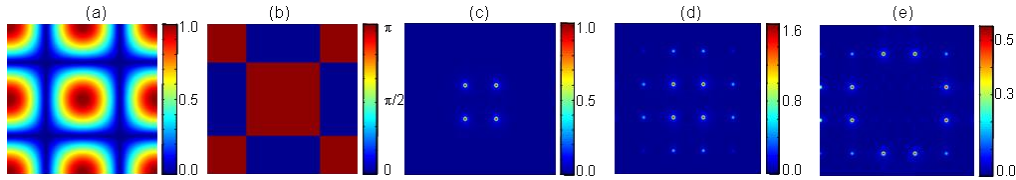


Fig. 3. (a) Modulus and (b) phase in the basic cell of the NDOF with parameters ( $Q = 4$ ,  $p = 0$ ) and a shift  $\pi/4$  in  $\theta$ . The Fourier spectra correspond respectively to (c) the NDOF  $h(x,y)$ , (d) the kinoform  $h_K(x,y)$ , and (e) the error function  $e(x,y) = h_K(x,y) - \beta h(x,y)$ .

In general, the NDOFs corresponding to numbers  $Q = 2, 3, 4$  and  $6$  of interfering plane waves, with arbitrary values of  $p$ , can be treated analytically or numerically. The reason is that these fields are periodic functions with either rectangular or hexagonal structures, whose basic cells can be easily obtained, at least by numerical computation. Another example corresponding to a periodic case is the NDOF with indices ( $Q = 6$ ,  $p = 1$ ). The amplitude in the basic cell of this NDOF has been shown at the center of Fig. 1(c) and the phase modulation of the kinoform, at the same domain, is displayed in Fig. 1(d). The Fourier spectra modules for the NDOF and its kinoform are displayed in Figs. 4(a) and 4(b). The complex amplitudes of the 6 brightest spots in the kinoform spectrum, computed using the kinoform basic cell, are proportional to the complex amplitudes of the corresponding 6 spots in the Fourier domain of the NDOF. The proportionality constant is  $\beta \approx 1.31$ . Using this value of  $\beta$  we compute the error function  $e(x,y) = h_K(x,y) - \beta h(x,y)$  and its Fourier spectrum  $E(u,v)$ . The modulus of  $E(u,v)$ , displayed in Fig. 4(c), shows null values in the space that corresponds to the spots of  $H(u,v)$ , fulfilling the kinoform spectrum condition.

For the numbers of interfering waves  $Q = 5$  and  $Q > 6$  the NDOF is quasi-periodic and it is not possible to obtain a basic cell to compute Fourier coefficients. However, it is still found, by numeric computation, that the kinoform Fourier spectrum contains spots that correspond to the Fourier spectrum spots of the NDOF. As an example, Figs. 5(a) and 5(b) show the Fourier spectrum modules of the NDOF with parameters ( $Q = 5$ ,  $p = 0$ ) and its kinoform. The amplitude gain that corresponds to the peak value of the spectrum modulus in Fig. 5(b), normalized to the peak value of the spectrum in Fig. 5(a), is  $\beta \approx 2.01$ . The phases in the bright kinoform Fourier spectrum spots are identical to those in the NDOF spectrum spots. Such numerically computed phases are shown in Figs. 5(c) and 5(d). Of course, the phase values in the kinoform spectrum only coincide with those of the NDOF spectrum at the positions of the bright spots. Similar results obtained for the NDOF with parameters ( $Q = 8$ ,  $p = 0$ ) and for its kinoform, are represented in Fig. 6.

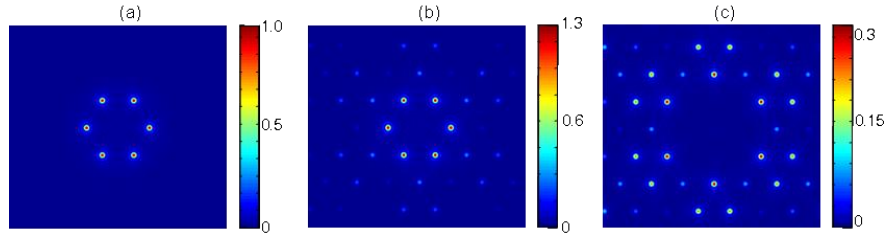


Fig. 4. Fourier spectra of (a) the NDOF  $h(x,y)$  with parameters ( $Q = 6$ ,  $p = 1$ ), (b) the corresponding kinoform  $h_k(x,y)$ , and (c) the error function  $e(x,y) = h_k(x,y) - \beta h(x,y)$ .

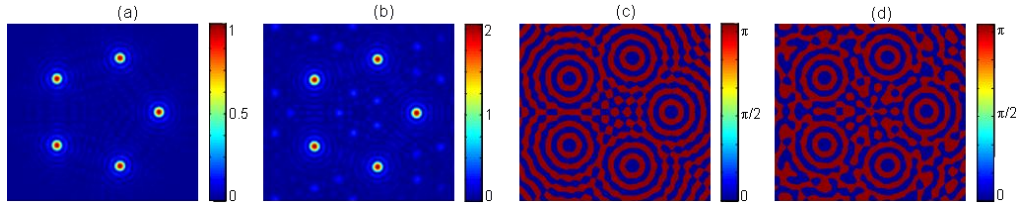


Fig. 5. Modules in the Fourier spectra of (a) the NDOF  $h(x,y)$  with parameters ( $Q = 5$ ,  $p = 0$ ), and (b) its kinoform  $h_k(x,y)$ . The phases of these Fourier spectra are respectively shown at parts (c) and (d) of the figure.

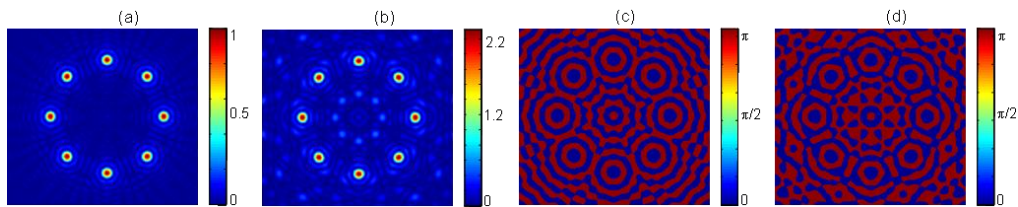


Fig. 6. Modules in the Fourier spectra of (a) the NDOF  $h(x,y)$  with parameters ( $Q = 8$ ,  $p = 0$ ), and (b) its kinoform  $h_k(x,y)$ . The phases of these Fourier spectra are respectively shown at parts (c) and (d) of the figure.

For the previously considered kinoforms we have shown the fulfillment of the kinoform spectrum condition. This result was proved analytically in the cases  $Q = 2$  and  $Q = 4$ . Moreover we have computed amplitude and efficiency gains that are larger than 1. The computed gains for several cases, including the already discussed ones, are presented in Table 1.

We obtained similar results for cases  $Q > 10$ . We proved numerically that it was still possible to fulfill the kinoform spectrum condition and therefore to generate the NDOF by means of its kinoform. The modules and phases of the Fourier spectra corresponding to the NDOF with parameters ( $Q = 25$ ,  $p = 0$ ) and for its kinoform, are displayed in Fig. 7. It is observed again that the phase values in the kinoform spectrum coincide with those of the NDOF spectrum at the positions of the bright spots. This fact enables the generation of the NDOF from the kinoform, by applying an appropriate binary filter in the Fourier domain of this phase element.

It is interesting to note that when the number of plane waves  $Q$  forming the NDOF is much larger than 10, the NDOF approximates to a non-diffracting Bessel beam whose order is equal to the parameter  $p$  [that determines the phase shifts  $\theta_n$  in Eq. (1)]. An illustration of this result is presented in Fig. 8 that displays the modules of the NDOFs with topological charge  $p = 1$ , and numbers of waves  $Q$  equal to 15, 30, and 50, respectively. As noted in this figure, the NDOF acquires the structure of a non-diffracting Bessel beam of order 1 when the number of interfering waves increases. A remarkable result that we proved analytically in a previous article [7], is that the kinoform of a non-diffracting Bessel beam of arbitrary order  $p$  fulfills

the spectrum condition and this field can be generated from its kinoform, by means of spatial filtering. In this case the required spatial filter is an annular sector. Therefore, the fulfillment of the spectrum condition for the kinoform of the NDOF in Eq. (1), when the number  $Q$  of interfering plane waves tends to infinity, is analytically confirmed in base of [7].

**Table 1. Amplitude and Efficiency Gains of Kinoforms for Several NDOFs**

NDOF Parameters ( $Q, p$ )	Amplitude Gain $\beta$	Efficiency Gain $\beta^2$
(2,0)	$4/\pi$	$16/\pi^2$
(3,0)	1.58	2.48
(3,1)	1.58	2.48
(4,0)	$16/\pi^2$	$256/\pi^4$
(5,0)	2.01	4.03
(6,0)	2.07	4.27
(6,1)	1.31	1.71
(7,0)	2.36	5.58
(8,0)	2.28	5.23
(9,0)	2.70	7.28
(10,0)	2.56	6.55

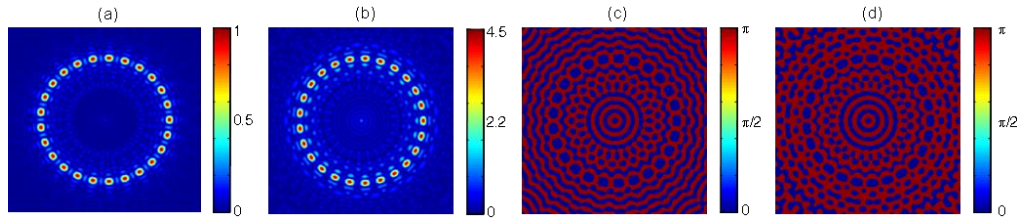


Fig. 7. Modules in the Fourier spectra of (a) the NDOF  $h(x,y)$  with parameters ( $Q = 25, p = 0$ ), and (b) its kinoform  $h_k(x,y)$ . The phases of these Fourier spectra are respectively shown at parts (c) and (d) of the figure.

We simulated numerically the generation of the NDOFs with indices ( $Q = 5, p = 0$ ) and ( $Q = 6, p = 1$ ) using their kinoforms. The process consisted in generating the Fourier spectra of the kinoforms and performing a spatial filtering on these Fourier spectra. The spatial filter is a binary mask that only transmits the Fourier spots corresponding to the term  $\beta H(u,v)$  and blocks out the spots corresponding to  $E(u,v)$ . The final step after the spatial filtering is an inverse Fourier transform. The modules and phases of the NDOFs generated with the described process are displayed in Fig. 9. These fields are quite similar to the exact NDOFs

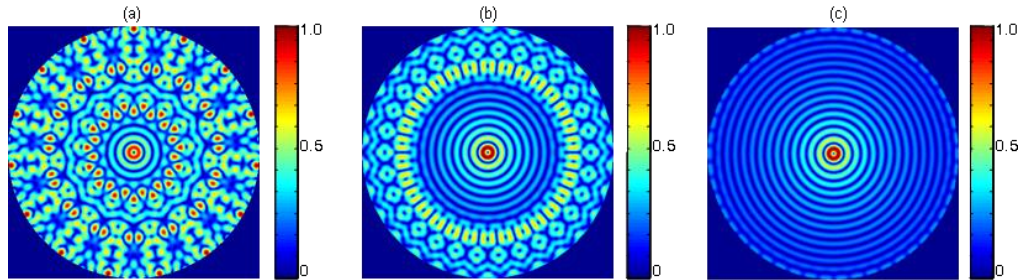


Fig. 8. Modules of the NDOFs with topological charge  $p = 1$  and number of interfering waves (a)  $Q = 15$ , (b)  $Q = 30$ , and (c)  $Q = 50$ . Note that the NDOF acquires the structure of a Bessel beam of order 1 when  $Q$  increases.

displayed in Fig. 1. Some minor field amplitude errors, appreciated e.g. at the borders of the fields in Figs. 9(a) and 9(c), are due to the finite size of both the pupil limiting the field and the small apertures that form the binary spatial filter employed in the simulations. Indeed, the finite pupil of the NDOF and its kinoform corresponds to a point spread function (PSF) in the

Fourier domain of these functions, which in practice allows only an approximate fulfillment of the kinoform spectrum condition. The influence of this finite PSF can be reduced by increasing the spatial frequency of the NDOF, which increases the distance between the spots in the Fourier domain, and reduces the mutual interference among these spots.

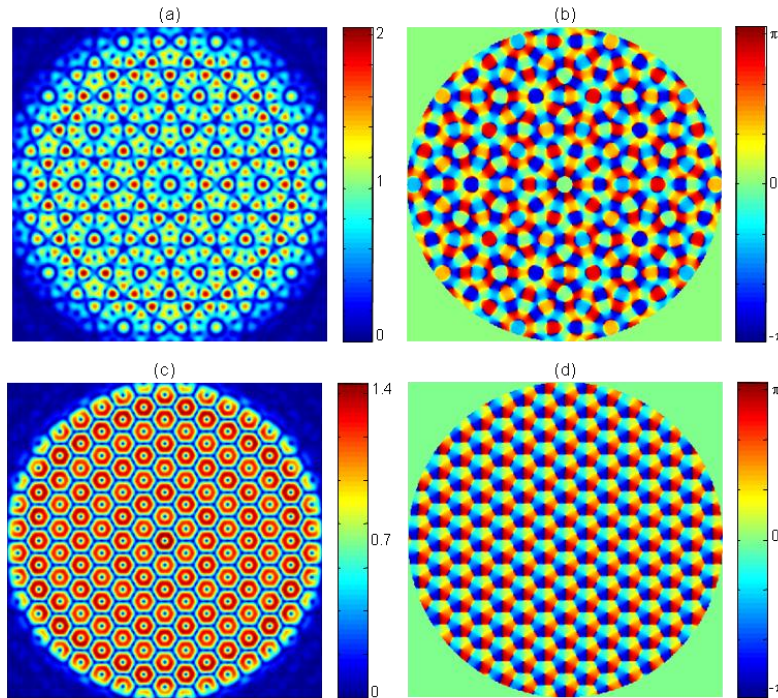


Fig. 9. (a) Modulus and (b) phase of a NDOF with parameters ( $Q = 5$ ,  $p = 0$ ), obtained by numerical simulation of the kinoform in a spatial filtering setup. The modulus and phase numerically obtained for the NDOF with parameters ( $Q = 6$ ,  $p = 1$ ), are respectively shown at parts (c) and (d) of the figure.

### 3. Experimental generation of a NDOF using its kinoform

We generated different NDOFs implementing their kinoforms with a pixelated phase SLM [21]. In the experimental setup, depicted in Fig. 10, the SLM is used in an oblique configuration. The laser beam (He-Ne,  $\lambda = 633$  nm) is conditioned by a beam expander (BE). Lenses ( $L_1$ ,  $L_2$ ) are employed to implement a double Fourier transform setup. The spatial filter (SF) blocks out the spots corresponding to  $E(u,v)$  in the Fourier spectrum of the kinoform. The implemented holograms are limited by a circular pupil whose diameter covers 512 pixels of the SLM. Since the SLM pixel pitch is 8 microns the pupil radius was  $R = 2048$   $\mu\text{m}$ . On the other hand, the multiple plane waves used in the specification of the NDOFs had a spatial frequency  $\rho_0 = 7.5$   $\text{R}^{-1}$ . Considering that the focal length of the Fourier transforming lens  $L_1$  was  $f_1 = 75$  cm, the spots in the Fourier domain corresponding to the encoded plane waves should appear at the distance  $r_0 = \lambda f_1 \rho_0 \approx 1738$   $\mu\text{m}$ , from the optical axis. Thus, the spatial filters were made of small circular holes with a common distance  $r_0$  to the axis. The diameter of the holes in the spatial filters was approximately  $r_0/2$  ( $\approx 870$   $\mu\text{m}$ ). The modules of the kinoforms Fourier spectra obtained experimentally and the generated NDOFs were computed from the intensities of these fields, recorded with a CCD. The modules of the experimental Fourier spectra of the kinoforms, for the NDOFs with indices ( $Q = 5$ ,  $p = 0$ ) and ( $Q = 6$ ,  $p = 1$ ), are displayed in Figs. 11(a) and 11(b). The modules of the NDOFs, obtained by performing the spatial filtering on the Fourier spectra of the kinoforms, are displayed in Figs.

11(c) and 11(d). These experimental results provide a confirmation of the theoretical and numerical results.

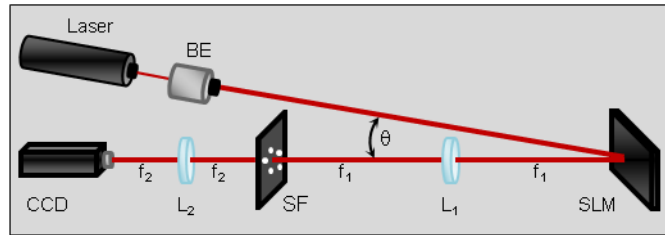


Fig. 10. Scheme of the experimental optical setup employed to generate a NDOF using its kinoform in a spatial filtering setup. The input laser beam, conditioned by the beam expander (BE) arrives to the phase SLM in an oblique direction.

#### 4. Conclusions and final remarks

We have discussed the generation of either periodic or quasi-periodic NDOFs, employing phase holograms, formed by the kinoforms of such fields. For the generation of the NDOFs, the phase holograms are employed in a double Fourier transforming setup with spatial filtering. This method allows the generation of the NDOFs with high accuracy and a remarkably high efficiency. The high performance of these holograms is due to the fact that the Fourier spectrum of the kinoform of a NDOF is formed by two disjoint parts, one of which is proportional to the Fourier spectrum of the NDOF itself. In fact, we have proved that the proportionality constant in this context is larger than unity, which is related to the high efficiency of the holograms. From a theoretical point of view, this is an interesting and unexpected result, since in general it is unlikely that the amplitude modulation  $a(x,y)$  of the complex NDOF  $f(x,y) = a(x,y)\exp[i\phi(x,y)]$  can be recovered by appropriate filtering using only the phase information  $\phi(x,y)$ . A comparison of the experimental results with the theoretical and numerical results provides a satisfactory verification of the described method.

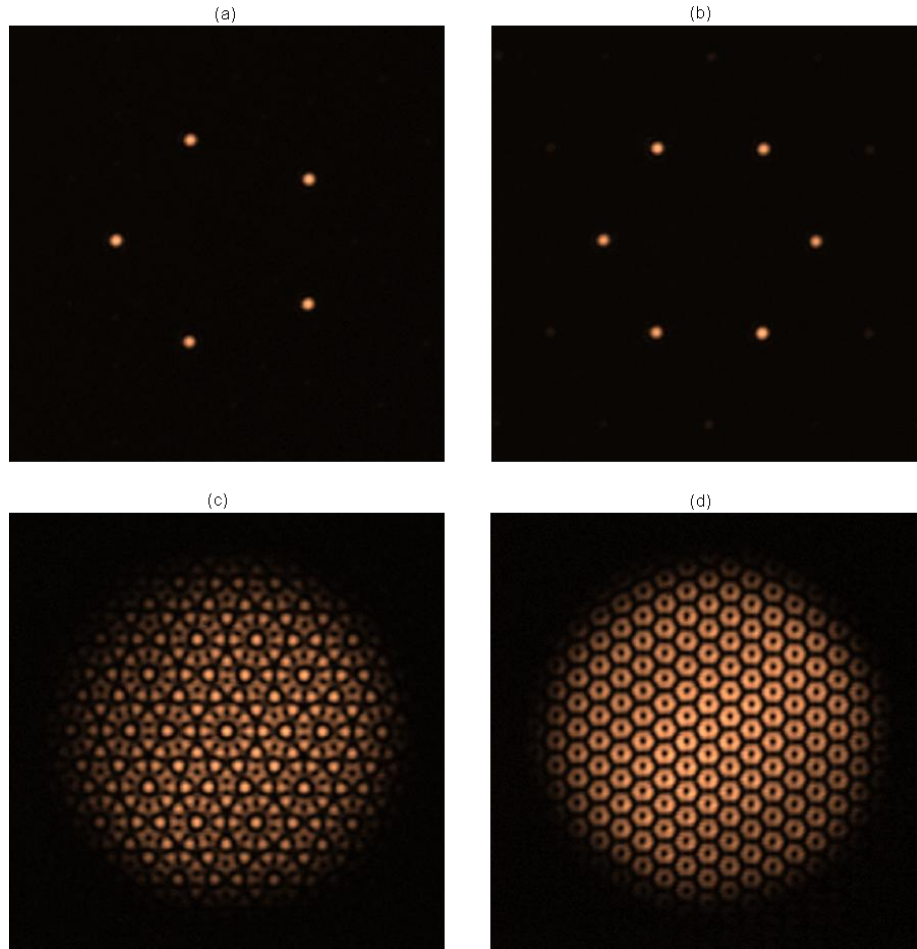


Fig. 11. Modules of the experimentally recorded Fourier spectra of the kinoforms for the NDOFs with indices (a) ( $Q = 5$ ,  $p = 0$ ) and (b) ( $Q = 6$ ,  $p = 1$ ). The modules of the respective experimentally generated NDOFs are displayed in the parts (c) and (d) of the figure.

### Acknowledgments

V. Arrizon acknowledges the financial support from CONACyT, Mexico, under the grant CB2005-24430/48744-F.